

Ising Pyrochlore Magnets: Low-Temperature Properties, “Ice Rules,” and Beyond

R. Siddharthan,¹ B. S. Shastry,¹ A. P. Ramirez,² A. Hayashi,³

R. J. Cava,³ and S. Rosenkranz⁴

¹Department of Physics, Indian Institute of Science, Bangalore 560012, India

²Bell Laboratories, Lucent Technologies, 600 Mountain Avenue, Murray Hill, New Jersey 07974

³Chemistry Department, Princeton University, Princeton, New Jersey 08540

⁴Materials Science Division, Argonne National Laboratory, Argonne, Illinois 60436

(Received 28 January 1999; revised manuscript received 15 March 1999)

Pyrochlore magnets are candidates for what Harris *et al.* [Phys. Rev. Lett. **79**, 2554 (1997)] call “spin-ice” behavior. We present theoretical simulations of relevance for the pyrochlore family $R_2\text{Ti}_2\text{O}_7$ (R = rare earth) supported by magnetothermal measurements on selected systems. By considering long-ranged dipole-dipole as well as short-ranged superexchange interactions, we get three distinct behaviors: (i) an ordered doubly degenerate state, (ii) a highly disordered state with a broad transition to paramagnetism, and (iii) a partially ordered state with a sharp transition to paramagnetism. Closely corresponding behavior is seen in the real compounds.

PACS numbers: 75.10.Hk, 75.25.+z, 75.40.Mg, 75.50.Lk

The pyrochlore rare earth titanates have attracted great attention recently because their unusual structure (the “pyrochlore lattice”) of corner-sharing tetrahedra can lead to geometric frustration and interesting low-temperature properties [1]. Our interest in these particular titanates was sparked by the observation that some of them are nearly ideal Ising systems [2–5]. Some intriguing experimental data presented below can be explained only by assuming a competition between classical dipole-dipole interactions and quantum superexchange. Depending on their relative magnitudes, the ground states of the Ising-like systems can be “ice-like,” ordered, or partially ordered. “Ice models” get their name because real (water) ice [6] has a large ground state degeneracy arising from local rules for the ordering of protons in water ice. Several related models have been studied since, involving nearest-neighbor Ising interactions; as far as we know, this is the first example where two competing interactions have been included in an ice-like model, with the physics changing significantly depending on their relative strengths.

Pyrochlores of the form $A_2B_2O_7$ have been extensively studied, where A are rare earth ions and B are transition metal ions, each forming interpenetrating pyrochlore lattices. Because A is trivalent and B is tetravalent, this allows occupation by a wide variety of magnetic species [7–9]. The lattice is a 3D version of the kagomé lattice (Fig. 1). We use a primitive unit cell with a tetrahedron as the basis. The tetrahedra form a face centered cubic lattice, so the structure can be viewed as four interpenetrating fcc lattices; a nonprimitive cubical unit cell is often used. Oppositely oriented tetrahedra are formed from the corners of these tetrahedra. The system can exhibit frustration, in both the isotropic Heisenberg antiferromagnet [8,10,11] and the Ising limit [2–5].

In our systems, the Ti^{4+} , like the O^{2-} ions, are non-magnetic. The rare earth A ion carries a large magnetic moment (from its unfilled f -electron shells), so that the

dipolar interaction is as significant as the superexchange. Another important aspect is the single ion anisotropy imposed by the crystal field (CF) interaction of D_{3d} symmetry at the rare earth site, since a strong easy-axis anisotropy results in the Ising limit, even for isotropic exchange interactions. Previous investigations of the low-temperature properties of these systems pointed out evidence for a strong single-ion anisotropy along the $\langle 111 \rangle$ direction, i.e.,

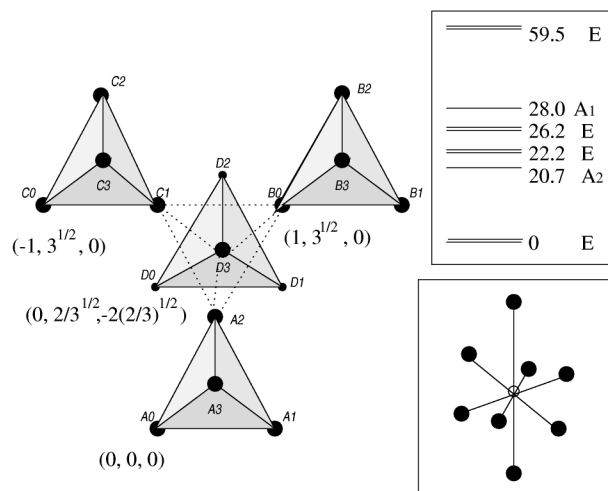


FIG. 1. The basis of atoms $A_0 = (0, 0, 0)$, $A_1 = (r, 0, 0)$, $A_2 = r(1/2, \sqrt{3}/2, 0)$, $A_3 = r(1/2, 1/[2\sqrt{3}], \sqrt{2}/3)$; translated by the lattice vectors $\mathbf{a}_1 = (r, \sqrt{3}r, 0)$, $\mathbf{a}_2 = (-r, \sqrt{3}r, 0)$, and $\mathbf{a}_3 = (0, 2r/\sqrt{3}, -2r\sqrt{2}/3)$ to form tetrahedra B , C , and D ; repeated translation forms the whole lattice. In our systems, $r = 3.53 \text{ \AA}$. We can also choose a basis of “downward” tetrahedra (dotted lines; atoms A_2, B_0, C_1, D_3). (inset bottom) A single rare earth ion (center) surrounded by eight oxygen ions. The top two are at the centers of the tetrahedra adjacent to the rare earth ion, and the rest form a puckered hexagonal ring around this axis. (inset top) The first few calculated energy levels for Ho, in meV, with symmetry indicated. Ground state transitions are observed at 22, 26, 59, 71, and 77 meV (the last two not shown).

along the line pointing from the center of the tetrahedron to the corner where the rare earth is located [2]. Direct evidence is provided by our detailed investigation of the CF interaction in the Ho compound using inelastic neutron scattering [12].

From the energies and intensities of the observed CF transitions, we could unambiguously determine the CF parameters and energy levels of $\text{Ho}_2\text{Ti}_2\text{O}_7$ (top inset to Fig. 1). Because the crystal structure varies very little on replacing one rare earth ion by another, these CF parameters will give good estimates of the splitting and single ion anisotropy in the other compounds as well. So we find a strong easy-axis anisotropy along the line joining the tetrahedra centers for Ho and Dy, but not for Yb, Er, or Tb.

Though it has been suggested earlier [3,13] that $\text{Yb}_2\text{Ti}_2\text{O}_7$ is also Ising-like, we find that it has an easy plane, rather than an easy axis: $J = 7/2$, $J_z = \pm 1/2$ for the ground states, so the spin points mainly in the x - y plane. The same seems to be true for Er, while Tb is Ising-like at low temperatures (< 10 K).

The nearest-neighbor Ising model on this lattice (considered in [2–4]) can behave in only two ways. If the interaction is “antiferromagnetic,” the ground state is doubly degenerate and each tetrahedron has either all spins pointing out or all spins pointing in, depending on the tetrahedron’s orientation. If the interaction is “ferromagnetic,” the ground state of a tetrahedron is given by an “ice rule” where two spins point out and two into the tetrahedron, and is sixfold degenerate. Any state with all tetrahedra satisfying this is a ground state. It is highly degenerate with a finite entropy per spin, which our simulations suggest is around $0.22k_B$ in agreement with Pauling’s prediction [14]. In both cases, the specific heat vanishes at small as well as large temperatures, with a peak in the middle. Simulations show that in the ferromagnetic case (ice rule) the peak is broad and occurs at the temperature scale of the interaction, suggesting a typical broad crossover from a glassy low-temperature phase with macroscopic entropy to a paramagnetic phase. In the antiferromagnetic case, the peak is very sharp and is at a temperature around 4 times the interaction energy, suggesting a phase transition from an ordered ground state to the paramagnetic phase. The energy scale of the peak here may be higher because of the higher energy cost of a single spin flip from the ground state.

Experiments were done on polycrystalline samples of these compounds which were synthesized from stoichiometric mixtures of the lanthanide oxides (99.99%) and TiO_2 (99.995%) heated at 1200°C in air for one week with intermediate grindings. All materials were found to be phase pure by conventional powder x-ray diffraction. The specific heat was determined using a standard semi-adiabatic technique and the susceptibility measured with a commercial magnetometer. All susceptibility data were taken at 0.1 T.

Specific heat measurements show very different kinds of behavior for these compounds. $\text{Dy}_2\text{Ti}_2\text{O}_7$ is the only one

whose behavior is akin to spin ice, as extensively discussed elsewhere [5]: the nearest-neighbor assumption seems to work well here. The possibility of ground state entropy from local ordering rules in an Ising model was discussed by Anderson as long ago as 1956 [15], but $\text{Dy}_2\text{Ti}_2\text{O}_7$ supplies a concrete real-world example with quantitative agreement with theory.

For Ho something entirely different happens: at around 0.6 K a transition seems to occur, below which the spins seem to decouple thermally from the system and freeze out into a low temperature metastable glassy phase. Moreover, the data for Ho suggest a peak at substantially smaller energies than the dipolar interaction (2.3 K). This is consistent neither with the ordinary spin ice nor with the antiferromagnet. To explain the difference in behavior between Ho and Dy, we need to go beyond the nearest-neighbor model, by (a) considering the long-ranged dipole-dipole interaction between the spins and (b) including an antiferromagnetic superexchange to reduce the dipolar coupling. It is not possible to account for the superexchange cleanly, so we merely assume that the superexchange is nearest neighbor only: this still gives us excellent agreement with the observations and highlights why these compounds are different from spin ice. We calculate the dipole-dipole interaction, assume a nearest-neighbor superexchange which we estimate from the experimental data, do a simulation for the specific heat and susceptibility with these values, and compare with experiment. Our simulations are on systems with 2048 spins ($8 \times 8 \times 8$ tetrahedra each with four sites) and around 10 000 Monte Carlo steps per spin. We use a long-ranged dipole-dipole interaction (up to five nearest-neighbor distances, but the results do not change significantly beyond the third neighbor). The convergence is good despite the long range of the interaction, probably because there is no global Ising axis and no net magnetization, so beyond the third neighbor the large numbers of spins in different directions tend to cancel one another.

We obtain the superexchange for Ho from the experimental high temperature zero field susceptibility. The high temperature expansion of the susceptibility is readily obtained from statistical mechanics. To fix the notation: we use scalar Ising spins, $S_i = \pm 1$, with $S_i = +1$ if it points out of an “upward” tetrahedron (or, equivalently, into a “downward” tetrahedron) and $S_i = -1$ otherwise. We write the first two terms in the expansion as $\chi(T) = \frac{C_1}{T} (1 + \frac{C_2}{T})$ and try to evaluate these coefficients using $M = \frac{1}{N} g_s \mu_B \langle \sum_i S_i \cos \theta_i \rangle$, where g_s is the Lande factor, S_i is the effective spin of rare earth atom i ($= \pm |J_z|$ for that atom), μ_B is the Bohr magneton, and θ is the angle made by the direction of the spin with the (arbitrarily chosen) direction of the external magnetic field. Our results turn out to be independent of the direction, at least to this order. The angle brackets denote the thermodynamic average. From the fluctuation-dissipation theorem, $\chi(T) = \frac{1}{N} \beta (g_s \mu_B)^2 \sum_{i,j} \Gamma_{ij}$, where $\Gamma_{ij} = \langle S_i \cos \theta_i S_j \times \cos \theta_j \rangle_{\mathcal{H}=0}$. Using standard methods (expanding to order

β), we arrive at

$$\chi(T) = \frac{N(g_s \mu_B)^2 S^2}{k_B T} \frac{1}{3} \left[1 - \frac{6S^2}{k_B T} \frac{1}{4} \sum_i \sum_j J_{ij} \cos \theta_i \cos \theta_j \right]$$

over one tetrahedron

The sum over j is over all sites in the lattice excluding i . If the nearest-neighbor dipolar interaction is J_D , the superexchange is J_S , and we include long-ranged dipolar interaction but only nearest-neighbor superexchange, we can write all the non-nearest-neighbor J_{ij} in terms of some constants times J_D . We get

$$\chi(T) = \frac{N(g_s \mu_B)^2 S^2}{k_B T} \frac{1}{3} \left[1 + \frac{6S^2}{k_B T} \frac{1}{4} (2.18J_D + 2.67J_S) \right]$$

and from here we can extract the coefficients C_1 and C_2 .

This is valid for an ideal Ising model at sufficiently high temperatures. When we plot the experimental χT against $1/T$ (Fig. 2), we find a marked linear region at low temperatures (2–10 K). This is the region we want: if we pull out C_2 from this region, we find it is much less than 1 K, so things are consistent. At higher temperatures, where the Ising approximation should fail, the graph is no longer linear. Using $C_2 = (6S^2/4)(2.18J_D + 2.67J_S)$ with J_D known, and the calculated value of C_1 , we can calculate J_S ; we get $J_D = 2.35$ K (calculated) and $J_S = -1.92$ K (measured). (Note that when we use scalar Ising spins rather than fixed vector spins, the superexchange is *negative* and the dipolar J_D is *positive*—and the former favors ordering, the latter frustration, as is usually the case in Ising systems.)

We now simulate with these values of J_D and J_S . In the case of $\text{Ho}_2\text{Ti}_2\text{O}_7$ (Fig. 3), the simulated susceptibility agrees well with the experimental data at all temperatures, while the specific heat has a sharp peak at very nearly the

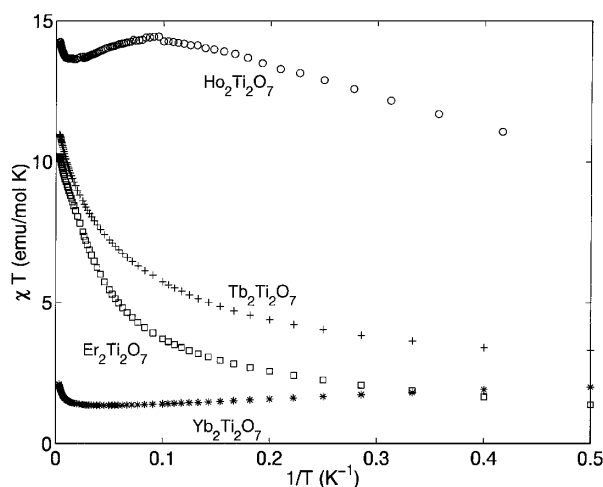


FIG. 2. χT plotted as a function of $1/T$. The high temperature expansion in the text is the markedly linear low temperature region here (2–10 K, which is high compared to C_2). Note that the Yb compound has the opposite slope here from Ho, suggesting that superexchange dominates here.

point where the experimental Ho system falls out of thermal equilibrium. Moreover, there is a large energy difference at this point, suggesting a first-order phase transition.

Contrary to earlier suggestions, the neutron data and our simulations suggest that the Yb and Er compounds are easy-plane (“XY models”), not Ising. Earlier work by Bramwell *et al.* [16] suggests that the XY Heisenberg model on this lattice shows a first-order phase transition from an ordered ground state; we believe that, as with $\text{Ho}_2\text{Ti}_2\text{O}_7$, it may be necessary to include a dipole-dipole interaction, and preliminary simulation of a pure dipole model correctly predicts the position and approximate shape of the peak. More work on this is in progress. Our specific heat measurements on Er and Yb agree with previous data [13].

The remaining compound, $\text{Tb}_2\text{Ti}_2\text{O}_7$, is probably Ising-like at very low temperatures. It has been suggested that it remains paramagnetic down to 0.07 K [17]. The gap to the excited CF states is only a few kelvin. The data for this and Er are shown in Fig. 4, but no simulations were done for these.

The ground states of nearest-neighbor ferromagnetic or antiferromagnetic Ising pyrochlores are well known; we now consider the more complicated case of $\text{Ho}_2\text{Ti}_2\text{O}_7$. In the nearest-neighbor ferromagnetic model any state in which all tetrahedra satisfy the ice rule will be a ground state. With long-ranged interactions ($\text{Ho}_2\text{Ti}_2\text{O}_7$), the ice rule remains but there are further restrictions on the allowed ground states. The simulation suggests a partial ordering in the ground state. That is, the upward tetrahedra

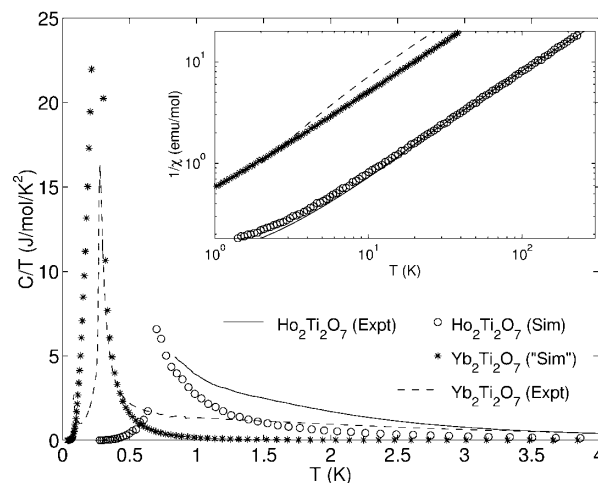


FIG. 3. Specific heat and (inset) dc susceptibility for $\text{Ho}_2\text{Ti}_2\text{O}_7$ and $\text{Yb}_2\text{Ti}_2\text{O}_7$. The Yb “simulation” here is for an Ising model, which is probably inappropriate but gives fair agreement.

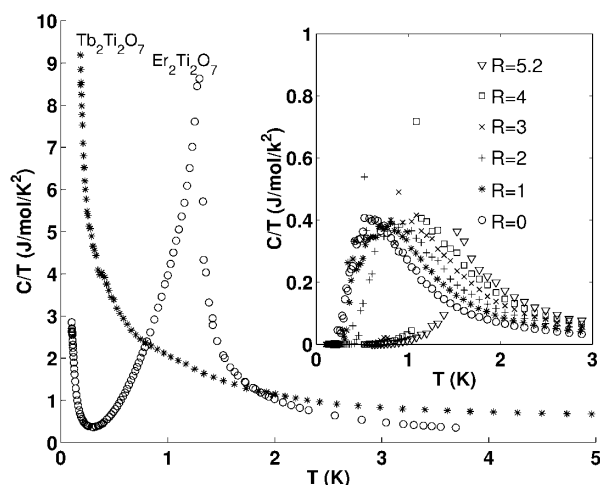


FIG. 4. The measured specific heat for $\text{Tb}_2\text{Ti}_2\text{O}_7$ and $\text{Er}_2\text{Ti}_2\text{O}_7$, and (inset) a comparison of simulations for the specific heat. Here the nearest-neighbor interaction is fixed and the numbers indicate the relative strength of the next-nearest interaction, relative to the pure dipole-dipole value. A pure dipole-dipole interaction has a nearest-neighbor J_D^1 and a next-neighbor J_D^2 , as well as further-neighbor interactions. In the presence of nearest-neighbor superexchange J_S , the nearest-neighbor interaction is reduced to $J_D^1 - J_S$. In this plot we normalize to a fixed energy scale for the near neighbor, so that the next-neighbor interaction is boosted by a factor $R = J_D^2 / (J_D^1 - J_S)$. Thus, $R = 1$ is the pure long-ranged dipole-dipole interaction (without superexchange), $R = 0$ is nearest neighbor only, and $R = 5.2$ is what we used for $\text{Ho}_2\text{Ti}_2\text{O}_7$. For $R = 0$ the ground state entropy is $0.22R$ in close agreement with Pauling. For $R = 1$ it decreases to $0.15R$, for $R = 2$ it is $0.12R$, and it further decreases as R increases; for large values, in particular, the value corresponding to $\text{Ho}_2\text{Ti}_2\text{O}_7$, it vanishes. A latent heat emerges at large values of R which must be accounted for in integrating these plots to find the entropy.

could have one of two allowed configurations; the configuration varies randomly along one lattice direction but alternates perfectly along the other two. Evidence from the simulations for this occurring is unambiguous. So the number of ground states is large but not macroscopic (it is exponential in L , the system length, rather than L^3), and the entropy per particle vanishes. Our calculation here ignored long-ranged superexchange, which would be present in the experimental system, but the experimental data for Ho do suggest a vanishing entropy for the ground state (on integrating C/T). In the simulation, the system remains in a disordered “paramagnetic” state till the transition temperature, but below this temperature it freezes out rapidly to such a partially ordered state. From then on further cooling leaves it stuck in this state, with the other ground states inaccessible. This seems to agree with the observation that the spins freeze in $\text{Ho}_2\text{Ti}_2\text{O}_7$ below a temperature of around 0.6 K. Below this temperature inability to establish thermal equilibrium leads to unreliable data, which has not been plotted here.

We believe the unusual freezing of spins in $\text{Ho}_2\text{Ti}_2\text{O}_7$ is because at the transition temperature (0.8 K) the single

spin flip energy is around 4 K, so the Boltzmann factor for this is very small (around 0.006). This spin freezing has been commented on by Harris *et al.* [2]. It seems the next-neighbor interactions must be fairly strong for this. In the absence of next-neighbor interactions there is a very large number of ground states. As we turn on and increase the next-neighbor interaction, the new constraints substantially reduce the ground state entropy. For a long-ranged dipole-dipole interaction without superexchange simulations suggest that the new ground state entropy is reduced by around 30% but still large, but with large superexchange, as in $\text{Ho}_2\text{Ti}_2\text{O}_7$, it actually vanishes: there are few true ground states, and these are separated by large energy barriers.

In summary, we perform simulations based on a theoretical calculation of dipole-dipole interactions and an estimated superexchange obtained from the experimental data. The relative strengths of these interactions have a drastic effect on the ground state properties when compared to a nearest-neighbor Ising model, and we observe three different kinds of ground states: highly disordered and ice-like [5], partially ordered, or fully ordered, with broad crossovers or sharp phase transitions to high temperature phases. We use only one adjustable parameter, fitted from the experimental data, as input for the simulations that agree well with experiment. Thus these systems look like excellent testing grounds to study the behavior of disordered spin systems, glassy dynamics, and phase transitions, with the opportunity to tune the interactions to some extent, and should richly repay future study.

We thank C. Dasgupta for helpful discussions. S.R.’s work was supported by U.S. DOE BES-DMS W-31-109-ENG-38.

- [1] A. P. Ramirez, *Annu. Rev. Mater. Sci.* **24**, 453 (1994).
- [2] M. J. Harris *et al.*, *Phys. Rev. Lett.* **79**, 2554 (1997).
- [3] M. J. Harris *et al.*, *Phys. Rev. Lett.* **81**, 4496 (1998).
- [4] S. T. Bramwell and M. J. Harris, *J. Phys. Condens. Matter* **10**, L215 (1998).
- [5] A. P. Ramirez *et al.*, *Nature (London)* **399**, 333 (1999).
- [6] J. D. Bernal and R. H. Fowler, *J. Chem. Phys.* **1**, 515 (1933); L. Pauling, *The Nature of the Chemical Bond* (Cornell University Press, Ithaca, 1945), p. 301.
- [7] J. E. Greedan *et al.*, *Phys. Rev. B* **54**, 7189 (1996).
- [8] B. D. Gaulin *et al.*, *Phys. Rev. Lett.* **69**, 3244 (1992).
- [9] J. E. Greedan *et al.*, *Phys. Rev. B* **43**, 5682 (1991).
- [10] R. Moessner and J. T. Chalker, *Phys. Rev. Lett.* **80**, 2929 (1998).
- [11] J. N. Reimers, *Phys. Rev. B* **45**, 7287 (1992); J. N. Reimers *et al.*, *Phys. Rev. B* **45**, 7295 (1992).
- [12] S. Rosenkranz *et al.* (unpublished).
- [13] H. W. J. Blote *et al.*, *Physica (Utrecht)* **43**, 549 (1969).
- [14] Anderson [15] supplies a version of Pauling’s argument for spin ice, giving the same answer: an entropy per spin of 0.20—within 10% of our simulation.
- [15] P. W. Anderson, *Phys. Rev.* **102**, 1008 (1956).
- [16] S. T. Bramwell *et al.*, *J. Appl. Phys.* **75**, 5523 (1994).
- [17] J. S. Gardner *et al.*, *Phys. Rev. Lett.* **82**, 1012 (1999).